Thermal Diffusivity Measurement of Isotopically Enriched 28-Si Single Crystal by Dynamic Grating Radiometry[1]

Y. Taguchi[2,3] and Y. Nagasaka[2]

It has been suggested in the past decade that the isotopic enrichment of 28-silicon increases the thermal properties. Thus, the 28-silicon is suitable for the heat sink of large-scale integrated circuits. Although some studies have been demonstrated on how to measure the thermal properties of isotopically enriched silicon, the accurate experimental data are not sufficient because of its high-conductivity and its large heat capacity which makes it difficult to measure. However, we have succeeded in developing the dynamic grating radiometry (DGR) to measure the thermal diffusivity of 28-silicon. In the DGR method, the sample is heated by interference of two pulsed laser beams, and the temperature decay is monitored by the infrared detector. By analyzing the temperature changes of the peaks and valleys of thermal grating, we can obtain the thermal diffusivity parallel and perpendicular to the sample surface simultaneously. In this paper, the optimum conditions of the experimental setup to measure the isotopically enriched silicon are discussed. The comparison of thermal diffusivities between 28-silicon and natural silicon (thickness is about 100μm) is presented, and the capability of DGR applied to isotope engineering is reported.

KEY WORDS: dynamic grating radiometry; high-conductivity thin film; isotope engineering; isotopically enriched 28-silicon; thermal diffusivity.

1. INTRODUCTION

In recent years, the thermal properties of electronic devices have become increasingly important for the thermal design of large-scale integrated circuits in which the density of heat sources increases exponentially (~100W·cm^{-2}). However, it is very difficult to measure the thermal properties of micro-scale device configurations (i.e. heat sinks and semiconductors) because of its high-conductivity and anisotropy that occurs in their production processes. Therefore, we have developed the dynamic grating radiometry (DGR) to measure anisotropic thermal diffusivity of high-conductivity films in the electronic circuits for *in-situ* condition. Also, we have reported the applicability of DGR to measure the orthotropic graphite sheet and highly oriented diamond film [1, 2].

In the isotope engineering [3], it is theoretically expected that the thermal properties of isotopically enriched 28-silicon (28-silicon: 99.924%) is superior to that of natural silicon. The isotopically enriched silicon can be applied as a substrate of ULSI for heat dissipation purpose. The mechanisms of phonon scattering in silicon are as follows: (1) scattering by the isotope (29-silicon and 30-silicon); (2) scattering by the sample boundary; (3) pointing defects or lattice imperfections; (4) obeying the normal process; and (5) obeying the Umklapp process. Thus, in the isotopically pure 28-silicon, the effect of isotopic composition

[1] Paper presented at the Fifteenth Symposium on Thermophysical Properties, June 22-27, 2003, Boulder, CO, U.S.A.

[2] Department of System Design Engineering, Keio University, 3-14-1, Hiyoshi, Yokohama, 223-8522, Japan.

[3] To whom correspondence should be addressed. E-mail: tag@naga.sd.keio.ac.jp

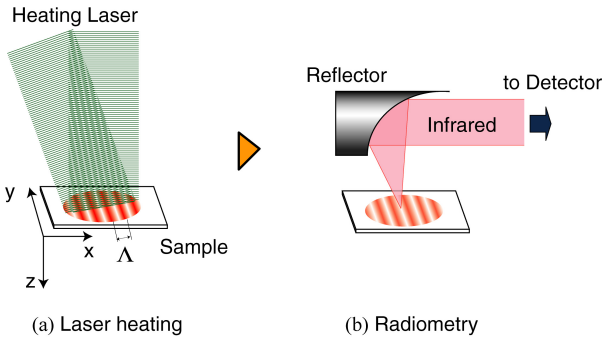

Fig. 1 The principle of DGR. (a) The sample is heated by the interference fringe pattern of two pulsed laser beams. The fringe space Λ is around 200~500μm. (b) The temperature distribution of sample is monitored via infrared thermometry as a function of two dimensional heat conduction.

(descending the scattering by the isotope) may affect the enlargement of thermal conductivity. However, the significant differences of thermal properties between 28-silicon and natural silicon have not been reported because of the difficulty of measuring silicon due to its small light absorption coefficient, large heat capacity, and its high conductivity. Moreover, there has been no contact-free technique to measure the thermal properties of semiconductors and insulators, which can be applied for the in-process control. Hence, the thermal properties measurement technique for *in-situ* is required to satisfy these demands.

In the present paper, the optimum experimental setups of DGR for measuring 28-silicon are reported. By using the focused Gaussian laser beam in the heating process, the heat loss toward the outside of the heating area and the influence of the oxidization are not negligible. In addition, the effect of signal/noise factor, which generates the dispersion and deviation of experimental results, is described. Finally, we will discuss the difference of results in the experiments between 28-silicon and natural silicon using DGR. The applicability of DGR to the isotope engineering is studied.

2. MEASUREMENT THEORY

In the DGR method, the sample is heated by the interference fringe pattern of two laser beams. The temperature change due to the two-dimensional heat conduction parallel and perpendicular to the sample is monitored as a change of infrared signal, see Fig. 1. To consider the two-dimensional heat conduction, we assume that the sample surface is uniformly heated by the laser grating instantaneously, and the boundaries of semi-infinite sample surface are adiabatic. In this case, the solution of two dimensional heat conduction equation is described as

$$T_{xz}(x,0,t)=\left\{T_0+T_1\exp\left(-\frac{t}{\tau_x}\right)\cos\left(\frac{2\pi x}{\Lambda}\right)\right\}\left\{\exp\left(\frac{t}{\tau_z}\right)\mathrm{erfc}\left(\sqrt{\frac{t}{\tau_z}}\right)+\Delta T_{\mathrm{f}}(0,t)\right\}, \tag{1}$$

$$\tau_x=\frac{1}{a_x}\left(\frac{\Lambda}{2\pi}\right)^2 \quad \text{and} \quad \tau_z=\frac{1}{a_z\alpha^2},$$

where T_0 is the mean initial temperature rise, T_1 is the spatially temperature distribution, Λ is the fringe space, and τ is the time constant of each direction, which are defined with the thermal diffusivities $a_{x,z}$ and light absorption coefficient α [1]. The $\Delta T_{\mathrm{f}}(0, t)$ is the temperature rise that occurs due to the effect of sample thickness [2].

However, it is impossible to determine both time constants in Eq. (1), because the equation is the product of two simple decays. By utilizing the pattern of sinusoidal temperature distribution, which is monitored by the scanning system of two laser beams, we are able to separate the thermal diffusivities parallel and perpendicular to the plane in Eq. (1). When the reflectors condense the emission from both extremes of the peaks and valleys of sinusoidal temperature distribution, the exact shape of temperature changes are expressed as

$$T_P = T_{xz}(0,0,t)\ ,\ T_V = T_{xz}(\Lambda/2,0,t)\,, \tag{2}$$

where T_P and T_V are the temperature decay of a peak and valley, respectively. Then, the heat conduction in the z- and x-direction are separated by using a peak and valley [Eqs. (2)] of thermal grating as follows:

$$T_z = \frac{1}{2}\{T_P(0,0,t) + T_V(\Lambda/2,0,t)\} = T_0\left\{\exp\left(\frac{t}{\tau_z}\right)\mathrm{erfc}\left(\sqrt{\frac{t}{\tau_z}}\right) + \Delta T_f(0,t)\right\}, \tag{3}$$

$$T_x = \frac{T_P}{(T_P + T_V)/2} = 1 + \frac{T_1}{T_0}\exp\left(-\frac{t}{\tau_x}\right). \tag{4}$$

By using the decay signals of temperature distribution of the two extremes (the peak and valley), the non-dimensional temperature change that includes information on the horizontal thermal diffusivity is determined by Eq. (4). Figure 2 illustrates (a) the typical temperature distribution of the results of scanning and the temperature changes at the extreme of thermal grating, and (b) non-dimensional temperature change analyzed by Eq. (4). Hence, in DGR, we can extract the thermal diffusivities parallel and perpendicular to the plane separately.

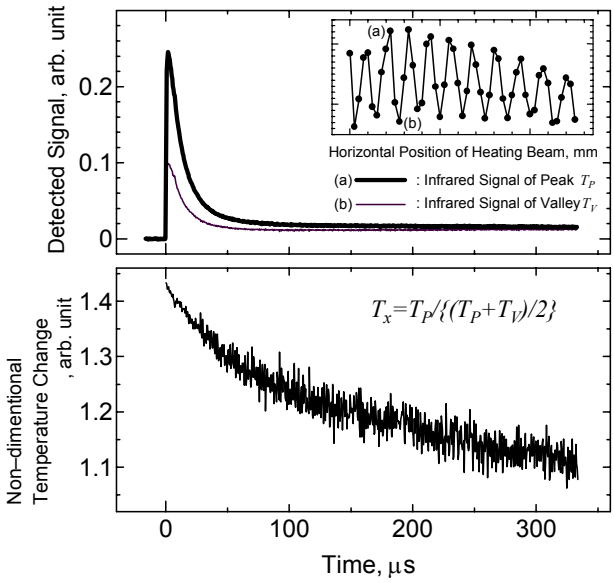

Fig. 2 A typical example of temperature change. Upper diagram: The inset shows the thermal grating detected by the scanning thermometry. (a) is defined as a peak and (b) as a valley of interference pattern. Lower diagram: Non-dimensional temperature change includes the information of heat conduction parallel to the sample surface.

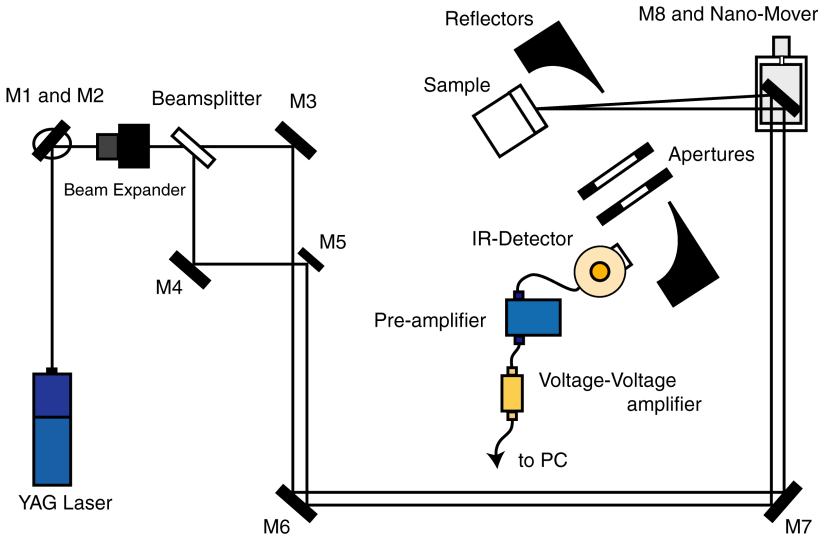

Fig. 3 Experimental apparatus of DGR.

3. EXPERIMENTAL APPARATUS

A schematic image of the present experimental apparatus is illustrated in Fig. 3. To create the transient thermal gradient instantaneously, a Nd:YAG Q-switched pulse laser (NEW WAVE Res.: power 50mJ·5ns^{-1} at 532nm wave length with a repetition rate up to 10Hz) is adopted. The beam expander, which has a diopteral controller, is employed to generate high-contrast sinusoidal temperature distribution on the sample surface that has a large heat capacity and a small absorption coefficient materials such as silicon. A pulsed high-power laser beam is divided by a beam splitter into two beams of equal intensity. Two beams are intersected on the sample surface by mirrors under an angle θ (θ is determined from the distance between M3 and M5) and generate an optical interference fringe pattern whose intensity distribution is spatially sinusoidal. In order to monitor the decay of temperature distribution caused by the heat conduction process, we employ infrared thermometry by measuring the thermal radiation emitted from a spot on the sample surface. The nano-order moving system, which shifts the position of the heated area on the sample, is adopted to scan the sample surface and to observe the exact shape of the interference fringe pattern. The off-axis paraboloidal mirrors (the spatial resolving diameter δ is estimated to be 80 to 100μm) condense the emission from a sample to LN_2-cooled HgCdTe infrared detector (Fermionics : PVA-500-20), and the weak signal is amplified by a current-voltage preamplifier (bandwidth of 20MHz) and voltage-voltage amplifier (cutoff frequency of 200MHz). The detected signal is averaged for a hundred laser pulses to significantly improve the S/N ratio.

4. OPTIMUM CONDITIONS FOR MEASURING SILICON

4.1. The effect of the Gaussian distribution of heating laser

For the purpose of measuring the thermal diffusivity parallel to the plane, it is postulated in the idealized theoretical condition that the sample is heated uniformly by pulsed-laser beam, and the effect of the irregular laser heating caused by the Gaussian laser distribution has not been considered. However, in the case of local area heating using TEM_{00} laser beam, especially $\Lambda \sim w/2$ (w : Gaussian radius of heating laser), the influence of heat loss toward the outside of the heating area is not negligible.

To solve the heat conduction equation, which is considered the Gaussian radius of heating laser, the

Green's function as the temperature at (*x, y, z*) at the time *t* is adopted [4]. The Green's function is most conveniently defined for the closed surface as the potential that vanishes over the surface. The assumptions of one-dimensional heat conduction parallel to the plane are as follows: (1) The sample is semi-infinite solid ($-\infty < x < \infty, 0 < z < \infty$). (2) There is no inner heat source in the sample. (3) The sample surface boundaries are adiabatic. In this case of horizontal heat conduction, the Green's function $G_G(x,t,;x',t')$ in a sample is given by

$$G_G(x,t;x',t') = \frac{1}{2\sqrt{\pi a_x (t-t')}}\left[\exp\left\{\frac{-(x-x')^2}{4a_x(t-t')}\right\}\right]. \tag{5}$$

The initial temperature distribution in the x-axis $\Psi_G(x)$ is given by the following equation.

$$\Psi_G(x) = \left\{1 + Vi\cos\left(\frac{2\pi x}{\Lambda}\right)\right\}\exp\left(-\frac{2x^2}{w^2}\right), \tag{6}$$

where *Vi* is the visibility of an interference fringe pattern. The exact profile of the temperature distribution in the x-axis is described as:

$$T_G(x,t) = \int G_G(x,t;x',0)\,\Psi_G(x')\,dx'$$

$$= \Gamma\left\{1 + Vi\exp\left(-\frac{W}{\tau_x}x\right)\cos\left(\frac{2\pi}{\Lambda}W x\right)\right\}, \tag{7}$$

where

$$\Gamma = \frac{w}{\sqrt{8a_x t + w^2}}\exp\left(-\frac{2x^2}{8a_x t + w^2}\right) \quad \text{and} \quad W = \frac{w^2}{8a_x t + w^2}. \tag{8}$$

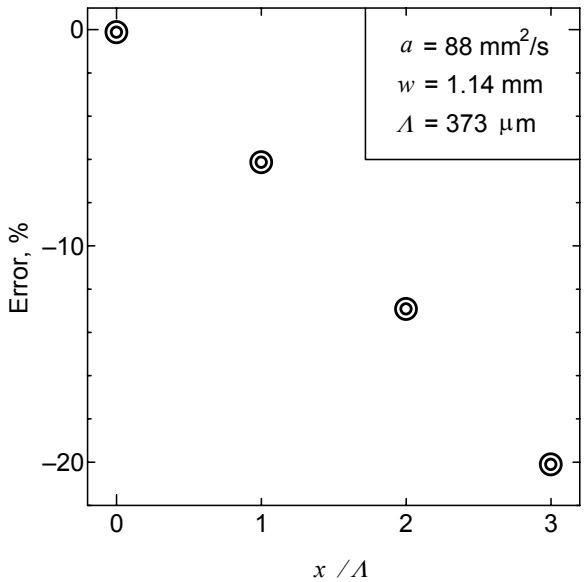

Fig. 4 The effect of Gaussian intensity distribution of heating laser beam as a function of $\Delta x/\Lambda$ at Λ = 373μm for a typical example of Gaussian radius w = 1.14 mm. Δx is the distance from the center of laser beam, and the error is calculated as the thermal diffusivity. error = $\left(a_{\text{fit}} - a_{\text{theory}}\right)/a_{\text{theory}} \times 100$.

According to the Eq. (7), the time constant τ_x and the fringe space Λ are expanded by W, and the span of detection time may affect directly to the result of curve fitting analysis. Using the procedure to separate the thermal diffusivities parallel and perpendicular to the plane (vide section 2), it will be complicated to estimate the error that occurs from heat leaking into the unheated region. To evaluate the thermal diffusivity error due to the Gaussian intensity distribution of heating laser, the numerical data, which is calculated by Eq. (7), is fitted by the ideal Eq. (4). Comparing the theoretical value and the results of curve fitting, the interrelationship between the effect of heat loss toward the outside of the heating area and the position of detected signals is confirmed. In Fig. 4, the error of the time constant is inverse proportional to the distance from the center of the heated area $\Delta x/\Lambda$. Thus, analyzing the signals of the peak and valley that are close to the center of the beam, we can eliminate the influence of the Gaussian irregular heating.

4.2. The effect of signal/noise factor

Fitting the signal that has a normal-mode noise, the white noise may have practically no influence to the results. In DGR method, for the purpose of reducing the background noise (e.g. background radiation, pointing stability of heating laser, and electronic noise), the infrared signal is electrically averaged for a hundred laser pulses (e.g. up to 40 dB at low signal of silicon) by digital storage oscilloscope. However, in the procedure to separate the thermal diffusivity parallel and perpendicular to the sample (see Eq. (4)), the influence of its noise is conspicuous. Moreover, it is predicted that the results of analysis may have dispersion or a deviation of the time constant and thermal diffusivity. In this section, the effect of noise factor is considered, and the optimum condition of averaging number is reported.

In order to estimate the dispersion or deviation of thermal diffusivity, the numerical model of temperature distribution including the normal-mode noise (based on the Eq. (7)) is considered. The numerical data (the peak and valley signal close to the center of heating area) are analyzed as non-dimensional temperature change by Eq. (4). Figure 5 illustrates the numerical simulation of natural silicon [5] based on Eq. (7) in various signal/noise ratio (S/N ratio). In the case of low S/N ratio (i.e. 30dB, 100 averaging), the analyzed thermal diffusivities are very widely dispersed. In addition, under these circumstances, the mean

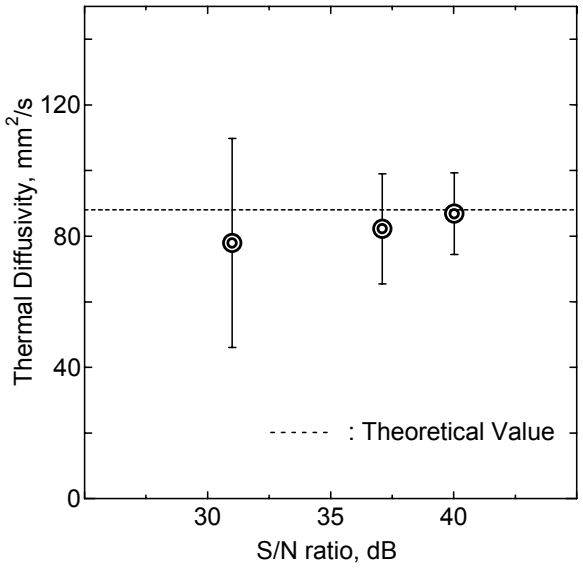

Fig. 5 The influence of noise factor. The numerical data that includes the normal-mode noise are analyzed by Eq. (3). The mean value of the thermal diffusivity parallel to the plane and the standard deviation are demonstrated.

thermal diffusivity is 12% smaller than the theoretical value. On the other hand, at high S/N ratio (i.e. 40dB, 1000 averaging), the dispersion of results is within 10%, and the deviation of mean value of thermal diffusivity is within around -2%. As mentioned above, whereas the deviation of mean thermal diffusivity is improved by increasing the S/N ratio, the reproducibility of fitting results is not dramatically improved. In the present work, the averaging points are set to ~1000 times to reduce the influence of noise factor.

5. RESULTS AND DISCUSSIONS

Natural silicon is composed of three different isotopes: 28-silicon (92.2%), 29-silicon (4.7%), and 30-silicon (3.1%). Takyu *et al.* [6] have successfully grown an isotopically enriched 28-silicon by using the gas centrifuge technique to separate 28-silicon stable isotopes, and the floating-zone method (FZ) for subsequent growth of an isotopically enriched bulk 28-silicon crystal. In this section, for the experimental investigation of the capability of increasing the thermal properties by isotopic enrichment, the specimens of 28-silicon and natural silicon (specifications are exhibited in Table I) are demonstrated.

To induce a high-contrast thermal image of the interference fringe pattern and achieve a high visibility of detected signal, a new optical system (i.e. laser focusing lenses and two apertures) and a new monitoring system (i.e. voltage-voltage amplifier and electrical averaging component) are utilized. A typical scanning image of silicon under a new experimental setup is illustrated in Fig. 6, and it shows the drastic improvement of modulation transfer function (MTF). Comparing the image of thermal grating with that of the optical image of a CCD camera, the spatial resolving power is estimated to be about 80μm.

Table I. Specifications of isotopically enriched 28-silicon.

	Thickness, μm	Composition of isotopes [Ref. 6]		
		28-silicon	29-silicon	30-silicon
natural silicon	(nominal) 130	92.2%	4.7%	3.1%
28-silicon	(nominal) 120	99.924%	0.073%	0.003%

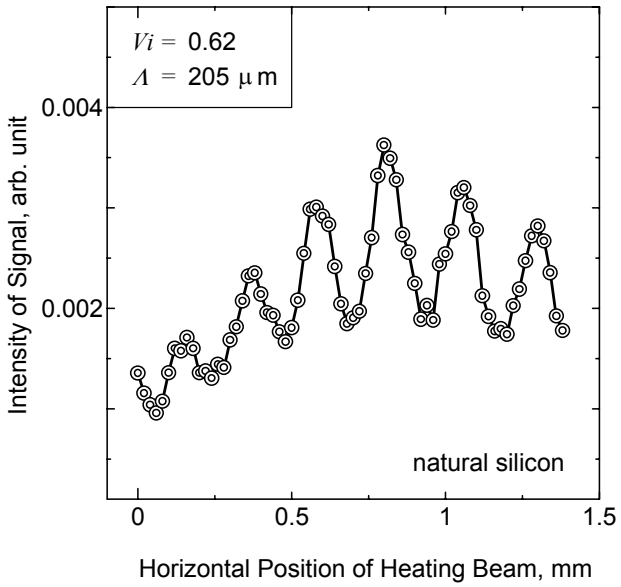

Fig. 6 The improvement of the contrast in the case of using the condense lens to increase the density of heating energy. The visibility of thermal grating is clearly increasing compared with the case of no-condense lens. The optical image is observed by CCD camera at once.

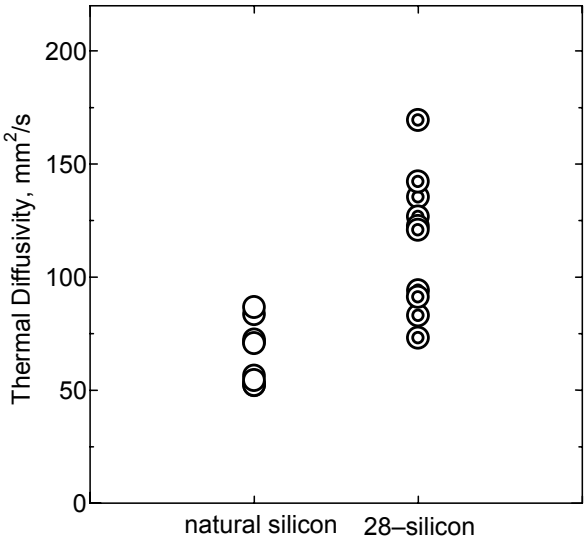

Fig. 7 The comparison of the experimental results of natural silicon and 28-silicon. The fringe space Λ=373μm and the Gaussian radius w=1.14mm. The results are dispersed by the noise factor (vide section 4.2).

Table II. Experimental results of natural silicon and 28-silicon.

	Thermal diffusivity, mm^2/s	Reproducibility
natural silicon	65.5	±20%
28-silicon	116	±26%

The experimental results of 28-silicon and natural silicon are summarized in Table II. Figure 7 compares the data for thermal diffusivity of natural silicon and 28-silicon. The signals of peak and valley are located at the center of laser beam in order to mitigate the effect of Gaussian temperature distribution with modeling described in section 4.1. First of all, attending to the results of natural silicon, the data spread of thermal diffusivity is within ±20%. As mentioned in section 4.2, in the condition of S/N = 38dB, the standard deviation is theoretically calculated as ±20% thus the experimental results are well agreed with the prediction by numerical simulation. Under such noisy conditions, according to Fig. 5, it was assumed that the mean value of thermal diffusivity would be 7% smaller than that of the recommended value. However, the deviation of the experimental results was slightly smaller than its predicted value. Due to the high power laser beam adsorption (i.e. silicon dioxide and carbon adsorber) and the emissive heat loss (silicon is transparent in near infrared region), the thermal diffusivity may have a tendency to be inferior to that of the predicted value. In DGR, considering the ideal condition of uniform laser heating, the emissive heat loss ΔT_{ems} in z-direction is expressed as

$$T_{xz}(x,0,t)=\left\{T_0+T_1\exp\left(-\frac{t}{\tau_x}\right)\cos\left(\frac{2\pi x}{\Lambda}\right)\right\}\left\{\exp\left(\frac{t}{\tau_z}\right)\mathrm{erfc}\left(\sqrt{\frac{t}{\tau_z}}\right)+\Delta T_{\mathrm{f}}(0,t)-\Delta T_{\mathrm{ems}}\right\}. \tag{9}$$

Thus, by using the procedure to separate the thermal diffusivity parallel and perpendicular to the sample (Eq. (4)), the heat loss ΔT_{ems} is negligible in a non-dimensional temperature change. Moreover, it is possible to reduce the effect of oxidization and adsorption by controlling the energy of the heating laser beam. In the case of 28-silicon, the S/N ratio of signal is estimated to be 40dB thus the dispersion of experimental results

is calculated as ±23% by numerical estimation (vide section 4.2). Therefore, we can confirm the significant difference of thermal diffusivity between 28-silicon and natural silicon. Itoh *et al*. [7] have numerically analyzed the thermal properties of isotopically enriched silicon, and they have indicated that the thermal conductivity of 28-silicon is 25% superior to that of natural silicon at room temperature. In the present work, the thermal diffusivity of 28-silicon was much larger than that of natural silicon, and the effect of isotopic enrichment of silicon was confirmed by DGR. Consequently, the applicability of DGR to isotope engineering was verified.

ACKNOWLEDGMENT

The authors would like to acknowledge Prof. K.M. Itoh of Keio University for supplying 28-silicon and exciting discussions. The work described in this paper was financially supported in part by the Science and Technology Agency under the Promotion System for Intellectual Infrastructure of Research and Development.

REFERENCES

1. Y. Taguchi and Y. Nagasaka, *Int. J. Thermophys*. **22**:1 (2001).
2. Y. Taguchi and Y. Nagasaka, *Trans. Jpn. Soc. Mech. Eng.* **B68**:665 (2002). (in Japanese)
3. M. Asen-Palmer, K. Bartkowski, E. Gmelin, M. Cardona, A.P. Zhernov, A.V. Inyushinkin, A. Taldenkov, V.I. Ozhogin, K.M. Itoh and E.E. Haller, *Phys. Rev*. **B56** (1997).
4. H.S. Carslaw and J.C. Jaeger, *Conduction of Heat in Solids*, 2nd Ed. (Oxford Univ. Press, London, 1959), pp. 449-460.
5. JSTP, *Handbook of thermophysical properties*, (YOKENDO, Tokyo, 1990), pp. 25. (in Japanese)
6. K. Takyu, K.M. Itoh, K. Oka, N. Saito, and V.I. Ozhogin, *Jpn. J. Appl. Phys*. **38**:12B (1999).
7. K.M. Itoh and K. Takyu, *Jpn. J. Appl. Phys*. **70**:10 (2001). (in Japanese)